Supporting Information

Thermo-Sensitive Hydrogels for Forward-Osmosis with NIR Light-Induced Freshwater Recovery

Xiang Xu, Haihui Li, Jiannan Cheng, Lifen Zhang,* and Zhenping Cheng*

Suzhou key Laboratory of Macromolecular Design and Precision Synthesis, Jiangsu Key Laboratory of Advanced Functional Polymer Design and Application; State and Local Joint Engineering Laboratory for Novel Functional Polymeric Materials; College of Chemistry, Chemical Engineering and Materials Science, Soochow University, Suzhou 215123, China.
E-mail: chengzhenping@suda.edu.cn (Z. P. Cheng), zhanglifen@suda.edu.cn (L. F. Zhang)

1. Testing and characterization methods of hydrogels.

To study the swelling ratio (SR) and water content (C_w) of hydrogels, we recorded the weight of hydrogels fully swollen in water and freeze-dried gels, and performed three sets of parallel experiments to minimize errors.

The SR of hydrogels within this period was calculated by Eq. (1):[1]

$$SR = \frac{w_s}{w_d} \#(1)$$

The C_w of hydrogels within this period was calculated by Eq. (2):[1]

$$Cw = \frac{w_s - w_d}{w_s} \#(2)$$

where w_s is the weight of the swollen hydrogels and w_d is the weight of the dry hydrogels.

The prepared hydrogels were used as draw agents to carry out the FO process on a homemade experimental platform as shown in Fig. S17 (a-d), ESI†. The FO membranes were kept in 0.5%-1.0% aqueous sodium metabisulfite solution, rinsed with deionized water, and soaked for 12 h before use. Afterward, they were mounted on the equipment platform and sealed with a rubber ring to prevent leakage. The FO membrane has a support layer facing the feed solution and an active layer facing the draw agents, with an active contact area of 1.33 cm^2. The feed solution was brackish water (2000 ppm NaCl) or DI water, and the draw agents were finely ground into small particles and filtered through a 100 mesh sieve with a size of ≈ 150 μm before use to ensure uniform particle size of the dry gel, which was then weighed to 0.03 g for FO testing. The FO process was carried out in a 5 °C environment for 8 h per cycle. The water flux (LMH) was calculated by Eq. (3):

$$LMH = \frac{V}{A \times t} \#(3)$$

where V is the volume (L) of water permeating through the membrane determined based on the mass increase of hydrogels after the FO process, A is the active contact area (m^2) between hydrogels and the active layer of the membrane, and t is the time (h) of the FO process.

The water recovery test is performed by scraping the hydrogel of the active layer at the end of the FO process and subsequently placing it in a transparent glass bottle and placing it in an oil bath at a certain temperature or in a ring-shaped NIR LED light source. The mouth of the clear glass bottle is connected to a vacuum pump via latex tubing (control vacuum expressed as 0.084 MPa), the interface is sealed with a sealing film and the gas wash bottle

in the ice bath is placed in the middle of the latex tubing to collect the water vapor (Fig. S12, ESI†). The water recovery rate (r) of hydrogels after the FO process was calculated by Eq. (4):[1]

$$r = \frac{w_r}{w_s - w_d} \#(4)$$

where w_r is the weight of recovered water.

The hydrogel cycling performance test is performed after the water recovery test. The hydrogel reuse ratio (R_r) was also calculated by Eq. (5):[2]

$$R_r = \frac{f_n}{f_0} \#(5)$$

where f_0 is the initial water flux of the initial run; f_n is the initial water flux after the N_{th} (N stands for 1-3) time of regeneration.

The crosslinking density of hydrogels is determined by the initial molar ratio of crosslinker to monomers, which is 10 mol% in this work.

2. Supplementary Schemes

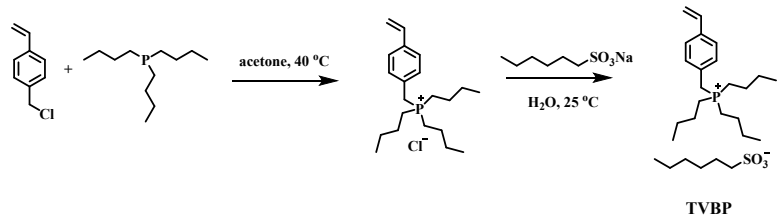

Scheme S1 Synthetic pathway of ionic liquid monomer TVBP

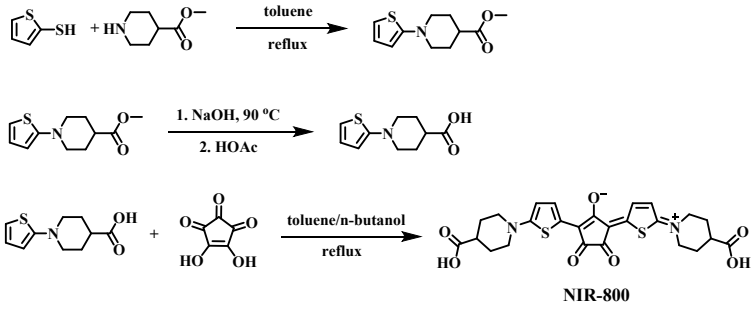

Scheme S2 Synthetic pathways of NIR-800

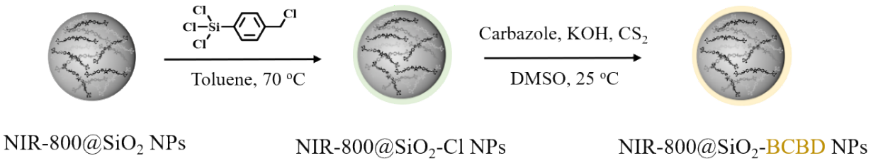

Scheme S3 Synthetic pathway of NIR-800@SiO_2-BCBD NPs (Surface modification methods according to Ref. [3])

3. Supplementary Figures

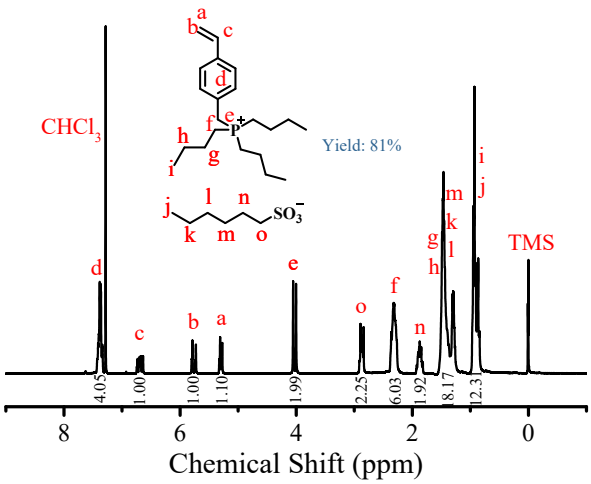

Fig. S1 ^{1}H NMR spectrum of TVBP in $CDCl_3$.

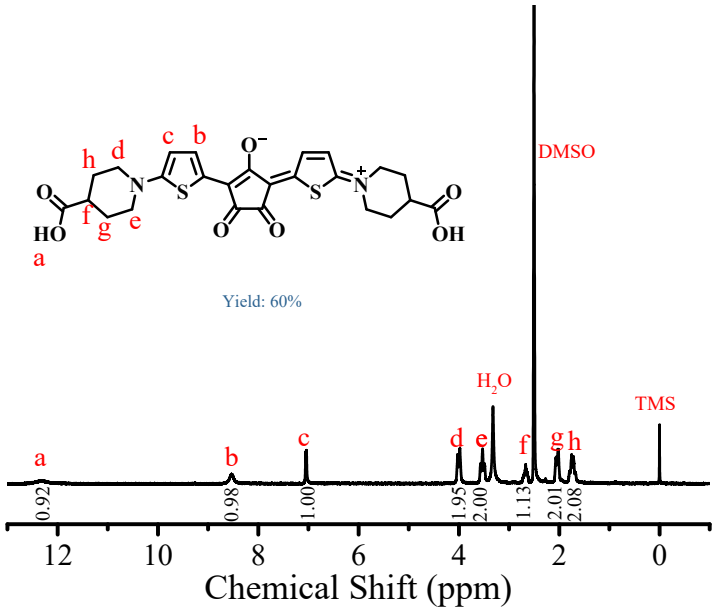

Fig. S2 ^{1}H NMR spectrum of NIR-800 in DMSO-d_6.

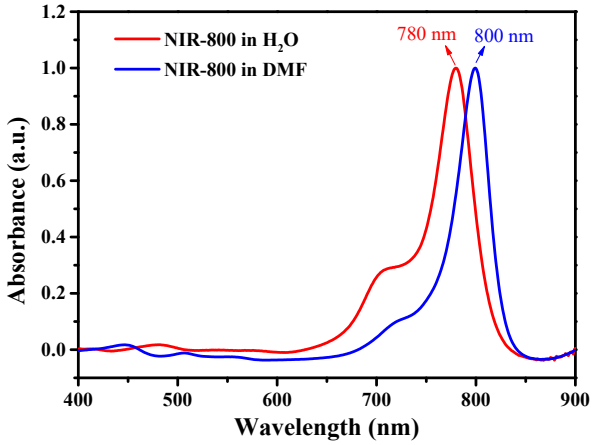

Fig. S3 UV-vis spectra of NIR-800 in H_2O and DMF.

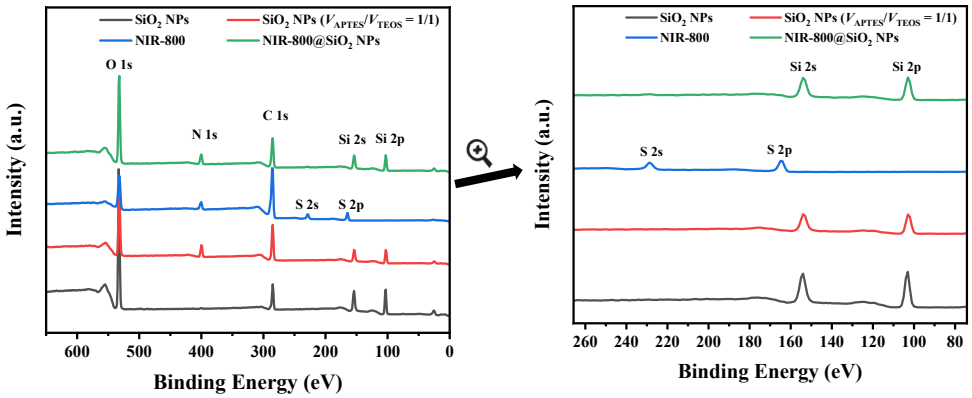

Fig. S4 XPS wide scan of SiO_2 NPs, SiO_2 NPs (V_{APTES}/V_{TEOS} = 1/1), NIR-800 and NIR-800@ SiO_2 NPs.

To demonstrate that NIR-800 is encapsulated inside the silica matrix and not on the surface, XPS was used for the analysis (Fig. S6). In pure SiO_2 NPs, SiO_2 NPs (V_{APTES}/V_{TEOS} = 1/1) and NIR-800@SiO_2 NPs, only Si, C, N and O elements are present. In contrast, the unique S element is present in NIR-800. Since the detection depth of XPS is only about a few nanometers, it can only detect the elements on the surface of the material. If NIR-800 was present on the surface of NIR-800@SiO_2 NPs, it would be detected by XPS as S element, but the opposite is true. It just proves that NIR-800 is completely encapsulated inside the silica.

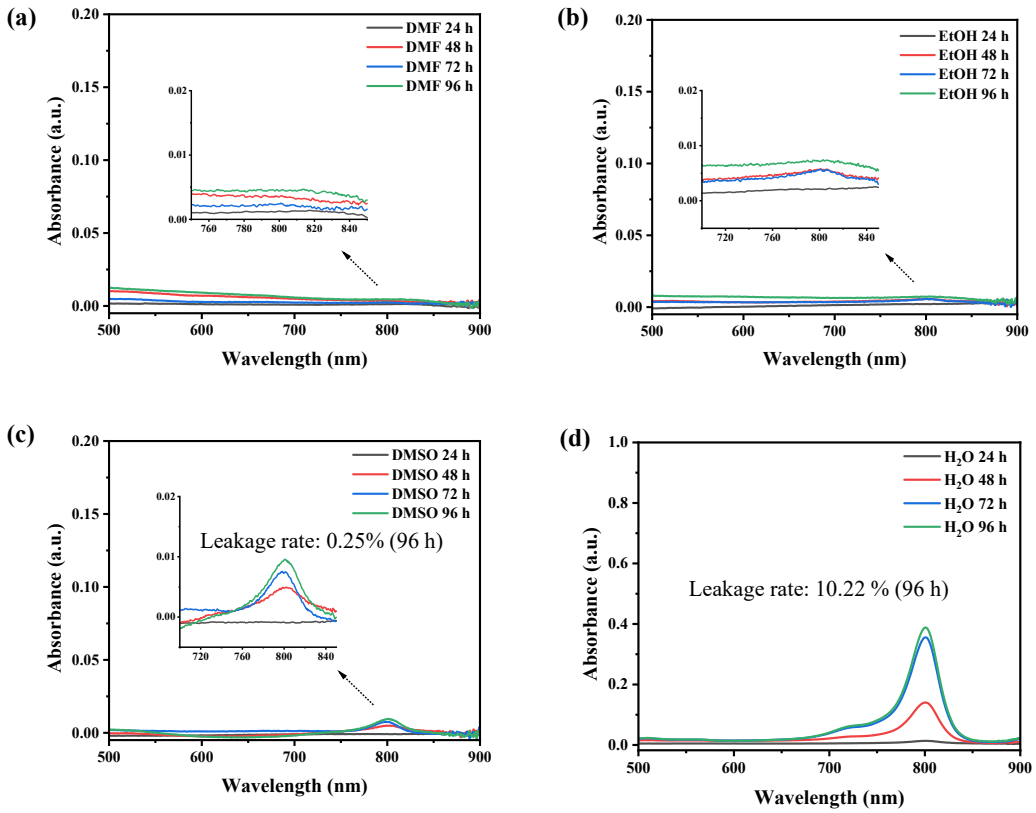

Fig. S5 UV-vis absorption spectra of leaked dye of NIR-800@SiO_2 NPs. The NPs were dispersed in (a) DMF, (b) EtOH, (c) DMSO and (d) DI water with vigorous stirring.

NIR-800@SiO_2 NPs (10 mg) were dispersed in each of the above solvents (2 mL). After a period of continuous vigorous stirring, 200 μL of the dispersion was removed and diluted to the same volume (3 mL) with DMF. After separating the NIR-800@SiO_2 NPs by centrifugation, the supernatant was taken for UV-vis test, and the leakage rate was calculated according to the standard curve shown in Fig. S6.

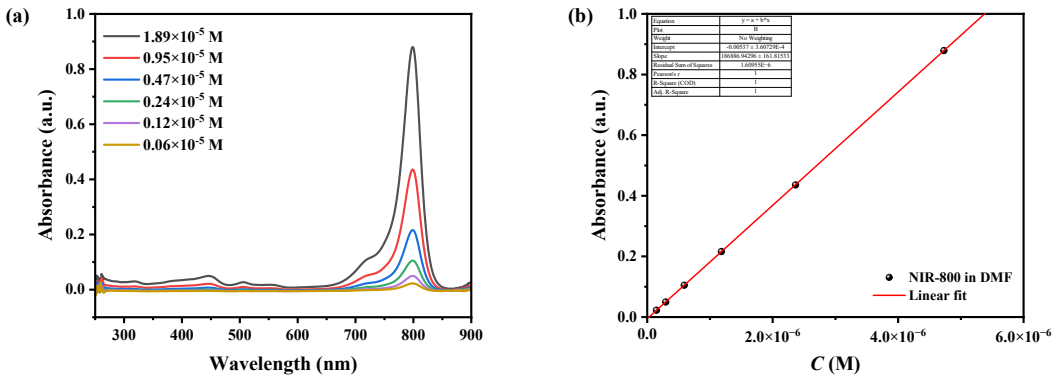

Fig. S6 Standard curve of NIR-800 in DMF.

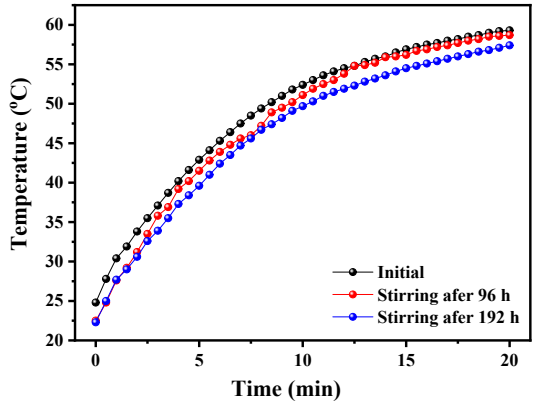

Fig. S7 Photothermal conversion curves of NIR-800@SiO_2 NPs (dispersed in water) after different stirring times, irradiation with NIR LED light (λ_{max} = 760 nm, 0.1 W/cm^2).

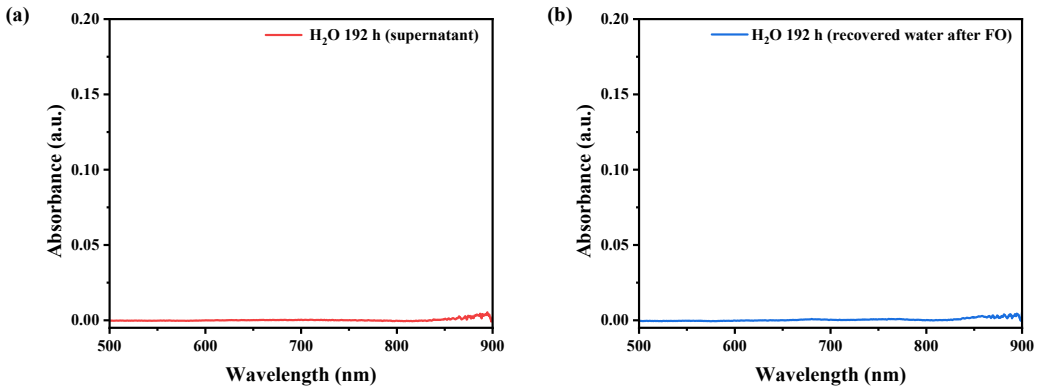

Fig. S8 UV-vis absorption spectra of leaked dye of NIR-800@SiO_2 NPs. (a) Supernatant of NIR-800@SiO_2 NPs after left in water for 192 h. (b) Water recovered from the hydrogel (NSPPH-22) after 192 h of FO.

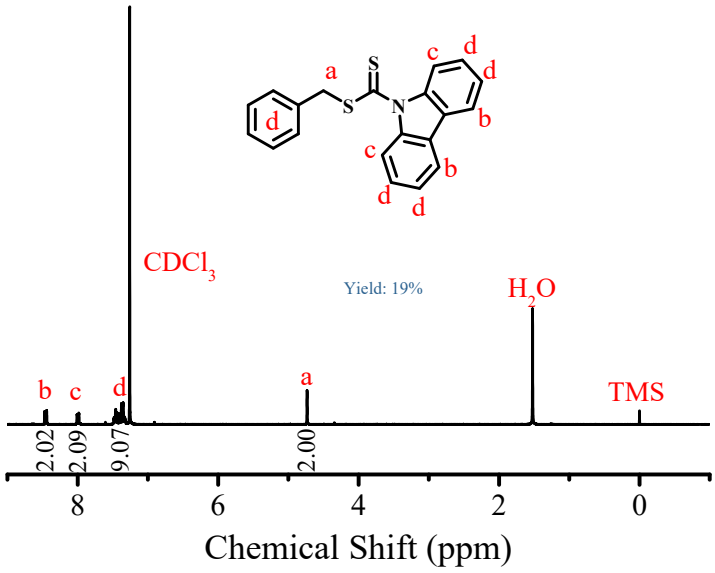

Fig. S9 ^{1}H NMR spectrum of BCBD in $CDCl_3$ (Synthesized according to Ref. [4]).

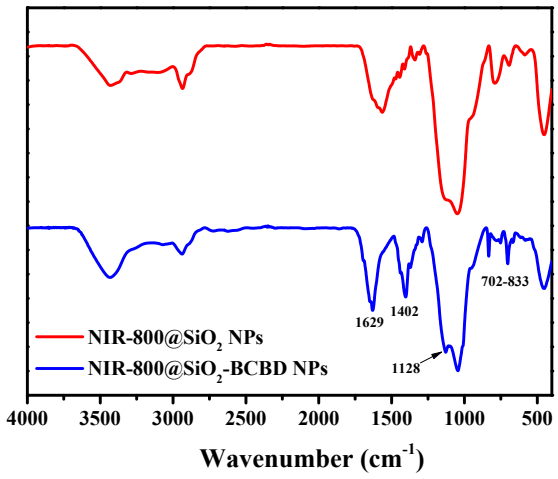

Fig. S10 FT-IR spectra of NIR-800@SiO_2 NPs and NIR-800@SiO_2-BCBD NPs.

The absorption peaks at 1629 cm^{-1} and 1402 cm^{-1} are attributed to the C=C stretching vibration of the benzene ring, the absorption peaks at 1128 cm^{-1} are attributed to C=S or -C-N-, and the absorption peaks at 720-833 cm^{-1} are attributed to the out-of-plane bending of the substituted benzene ring.

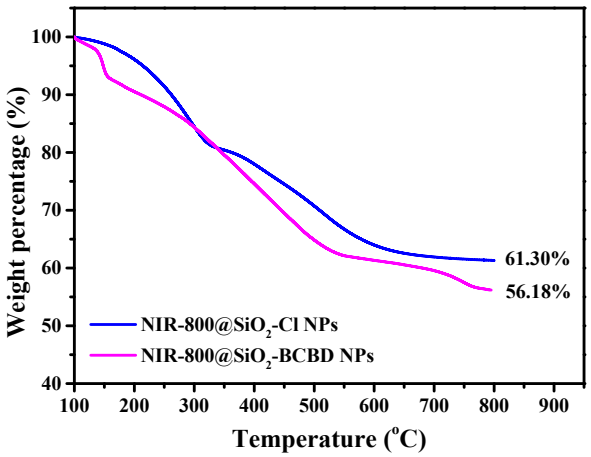

Fig. S11 TGA analysis of NIR-800@SiO_2-Cl NPs and NIR-800@SiO_2-BCBD NPs.

We calculated the content of BCBD on the surface of NPs by thermogravimetric analysis, which was about 0.2475 mmol/g.

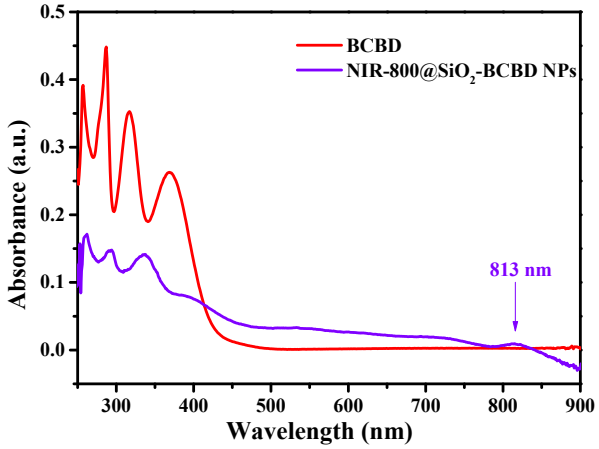

Fig. S12 UV-vis spectra of BCBD and NIR-800@SiO_2-BCBD NPs in DMSO.

The successful modification of BCBD on the nanoparticle surface can be further demonstrated by comparing the UV-vis absorption spectra of BCBD and NIR-800@SiO_2-BCBD NPs. The absorption peak at 813 nm can be attributed to the absorption of NIR-800.

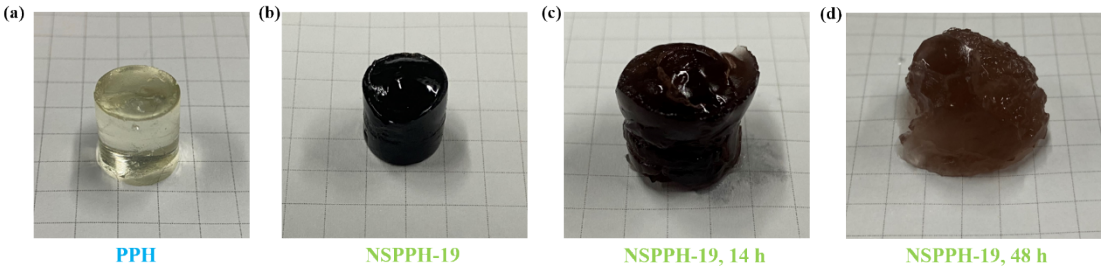

Fig. S13 Photographs of hydrogels. (a) PPH and (b) NSPPH-19 right after polymerization; NSPPH-19 after swelling in DI water at room temperature for (c)14 h and (d) 48 h.

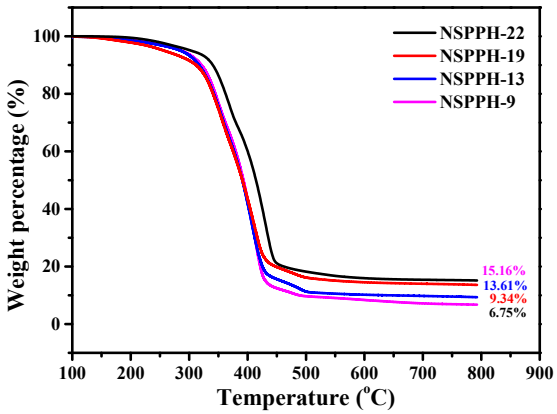

Fig. S14 TGA analysis of NSPPH hydrogels with different amounts of NIR-800@SiO_2-BCBD NPs.

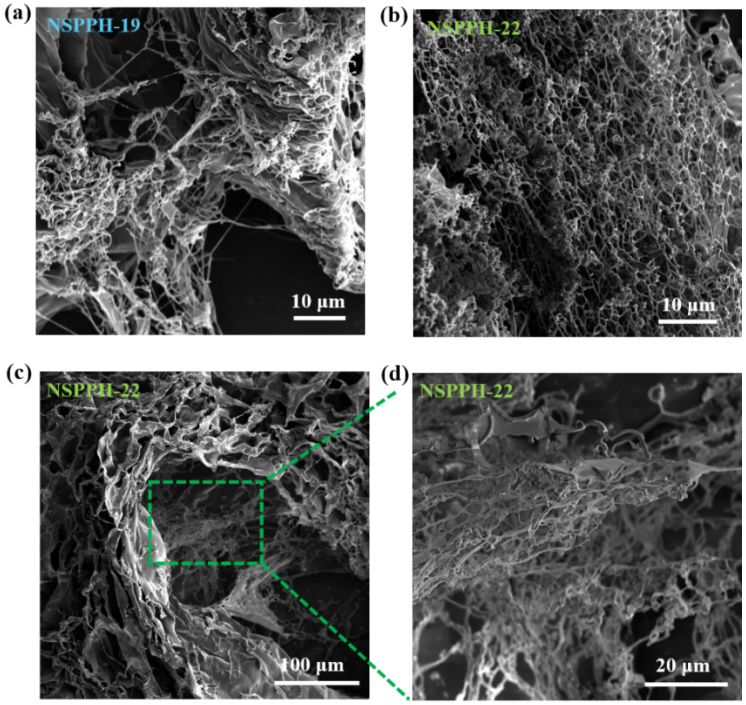

Fig. S15 SEM images of (a) NSPPH-19, (b-d) NSPPH-22. Where (b) and (c-d) are images of different positions of NSPPH-22, and (d) is a local enlargement of (c).

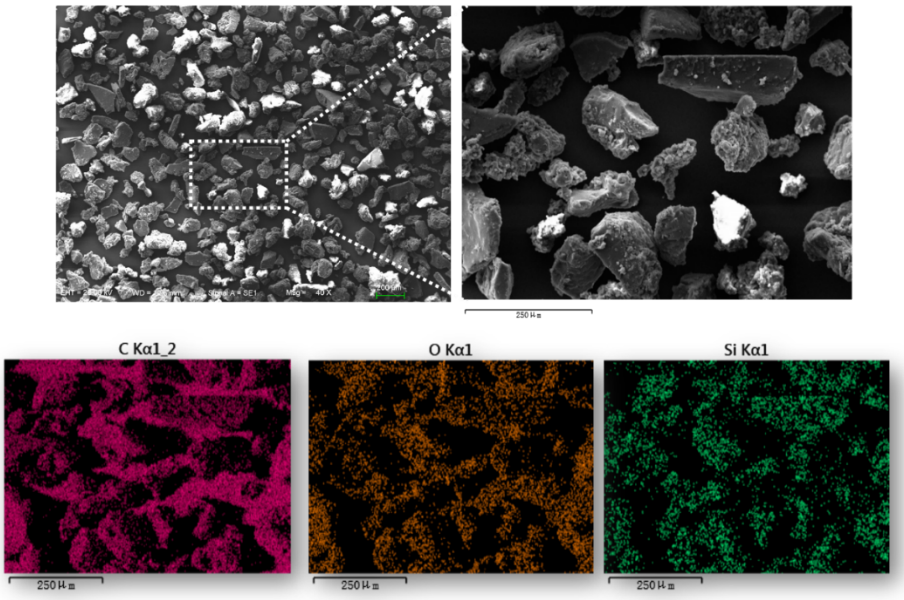

Fig. S16 EDS mapping images of NSPPH-13.

The hydrogels were dried and then ground for SEM mapping characterization. It can be seen from the pictures that the Si elements are uniformly distributed in the hydrogel particles, indicating that the nanoparticles are successfully doped into the hydrogel uniformly by SI-RAFT polymerization, which improves the drawback of physical co-mixing inhomogeneity.

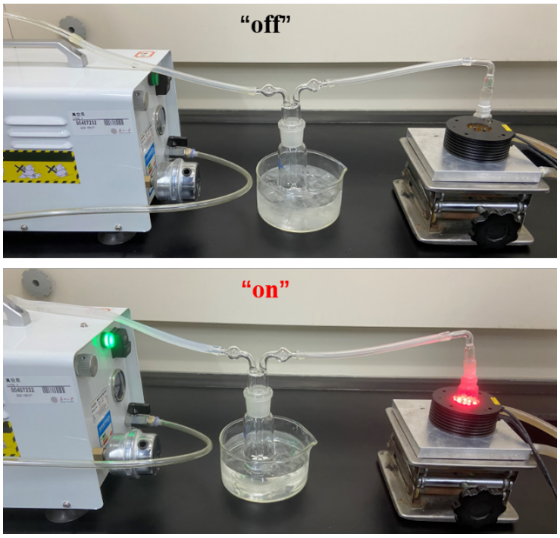

Fig. S17 Photographs of device for water recovery testing. From left to right are the vacuum pump, gas wash bottle and NIR LED light source.

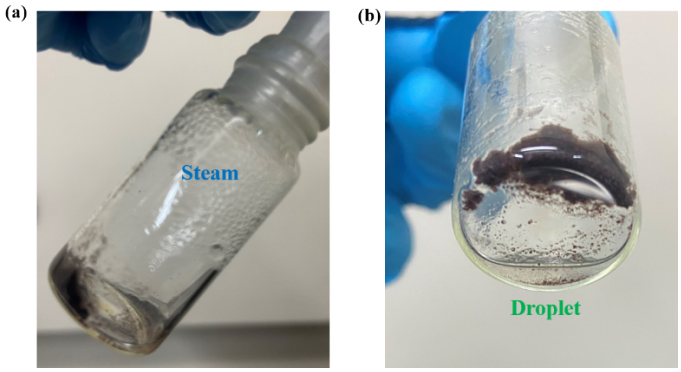

Fig. S18 Photographs of the hydrogel samples inside the bottles after 30 minutes of water recovery testing.

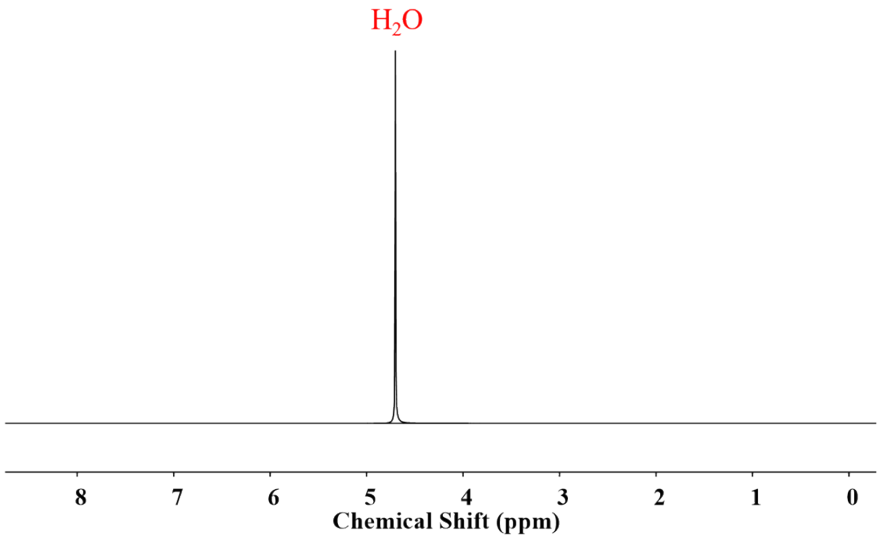

Fig. S19 ^{1}H NMR spectrum of recycled water in D_2O.

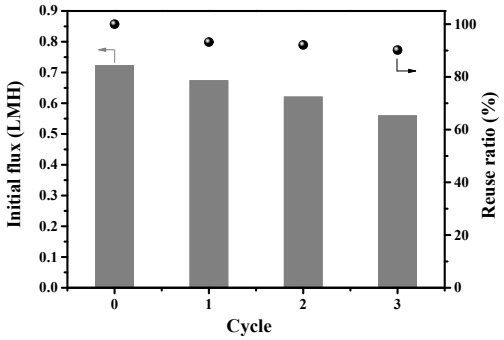

Fig. S20 NSPPH-22 was used as an example for the hydrogel cycle performance test. The water recycling was performed at a NIR light intensity of 0.2 W/cm^2.

The reusability data (reuse ratio) showed that after the first, second and third cycles, the reusability reached 93.22%, 92.11% and 90.18%, respectively, which means that after the third cycle, our hydrogels were still able to obtain about 77% of the initial effect.

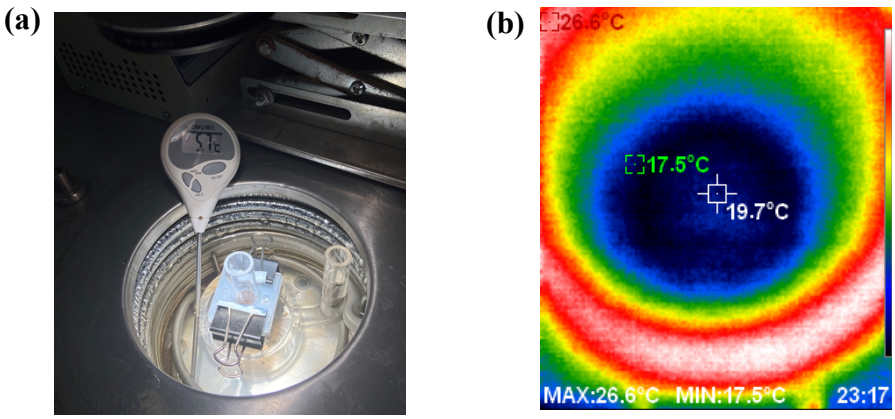

Fig. S21 (a) Photograph of the device under sunlight for FO, with a test environment of about 5 °C. (b) Thermal image of the apparent temperature of the hydrogels after 8 hours of continuous FO testing.

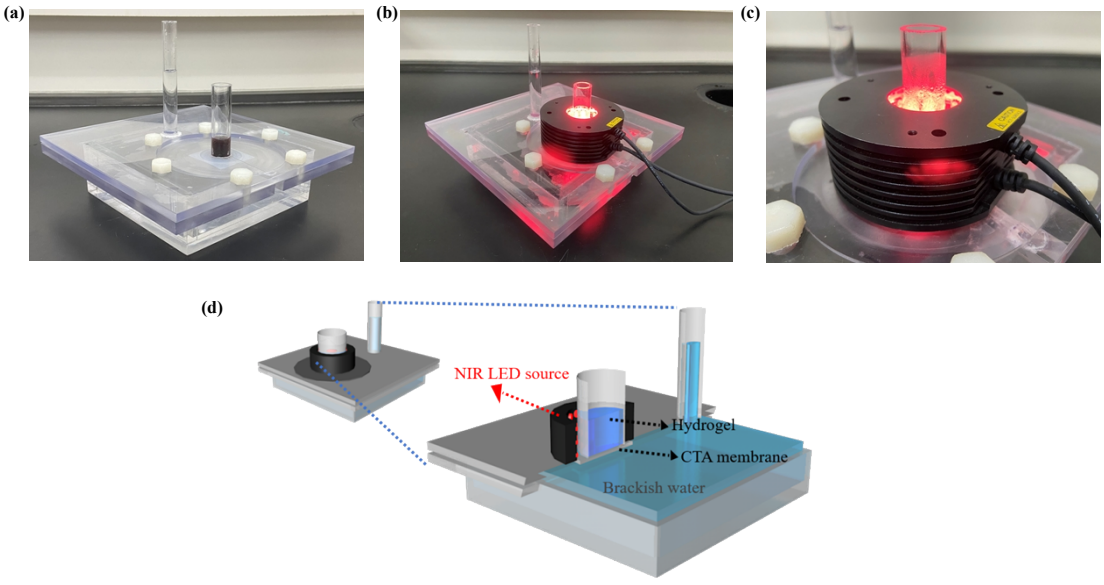

Fig. S22 (a) Effect of dry gel powder (0.20 g) after FO process (20 h) on a homemade desalination platform. (b) NIR LED light source was placed on the homemade platform and turned on for water recovery. (c) Steam appears and condenses in the tube during the water recovery process. (d) Structure diagram of homemade desalination platform.

4. Supplementary Tables

Table S1 Quantitative analysis of chemical composition of hydrogel samples.

Sample	NIR-800@SiO_2-BCBD NPs, wt.% (feed ratio to monomers)	[a]NIR-800@SiO_2-BCBD NPs, wt.% (feed ratio to all components)	[b]NIR-800@SiO_2-BCBD NPs, wt.% (actual ratio to all components)	[c]Conversion, % (reacted monomer)
NSPPH-9	8.8	6.5	12.0	51.2
NSPPH-13	13.0	9.4	16.6	51.8
NSPPH-19	19.0	13.1	24.2	47.2
NSPPH-22	22.0	14.8	27.0	47.3

***a*:** All components represent monomers, crosslinker and NPs.

***b*:** Calculated by TGA results, according to Eq.: $m_{NPs}/(m_{monomers+crosslinker}$*conversion+$m_{NPs})$

***c*:** Taking NSPPH-9 as an example, calculated by Eq.: (m_{NPs}*0.5618/0.0675-m_{NPs})/$m_{monomers+crosslinker}$, where 0.5618, 0.0675 represent the weight retention of NIR-800@SiO_2-BCBD NPs and NSPPH-9 at 800 °C, respectively (see Fig. S11 and S14 for TGA data).

References

1. X. Fan, H. Liu, Y. Gao, Z. Zou, V. S. Craig, G. Zhang and G. Liu, *Adv. Mater.*, 2016, **28**, 4156-4161.
2. Z. Pan, H. Guo, H. Yu, G. Wen, F. Qu, T. Huang and J. He, *Desalination*, 2021, **512**, 115147.
3. J. L. Liu, L. F. Zhang, S. P. Shi, S. A. Chen, N. C. Zhou, Z. B. Zhang, Z. P. Cheng and X. L. Zhu, Langmuir, 2010, 26, 14806-14813.
4. D. Zhou, X. L. Zhu, J. Zhu, L. H. Hu and Z. P. Cheng, *J. Appl. Polym. Sci.*, 2007, **103**, 982-988.